Geochemistry
Geophysics
Geosystems
AN ELECTRONIC JOURNAL OF THE EARTH SCIENCES
Published by AGU and the Geochemical Society

Article
Volume 10, Number 7
23 July 2009
Q07U06, doi:10.1029/2008GC002367
ISSN: 1525-2027

Holocene interdependences of changes in sea surface temperature, productivity, and fluvial inputs in the Iberian continental shelf (Tagus mud patch)

Teresa Rodrigues
Department of Marine Geology, INETI, Estrada da Portela-Zambujal, Apartado 7568, P-2721-866 Amadora, Portugal (teresa.rodrigues@ineti.pt)

Institute of Environmental Assessment and Water Research, CSIC, Jordi Girona, 18, E-08034 Barcelona, Catalonia, Spain

Joan O. Grimalt
Institute of Environmental Assessment and Water Research, CSIC, Jordi Girona, 18, E-08034 Barcelona, Catalonia, Spain

Fátima G. Abrantes
Department of Marine Geology, INETI, Estrada da Portela-Zambujal, Apartado 7568, P-2721-866 Amadora, Portugal

Jose A. Flores
Department of Geology, Faculty of Sciences, University of Salamanca, E-37008 Salamanca, Spain

Susana M. Lebreiro
Department of Marine Geology, INETI, Estrada da Portela-Zambujal, Apartado 7568, P-2721-866 Amadora, Portugal

Now at Department of Geosciences Research and Prediction—Global Change, Spanish Geological and Mining Institute, c/Ríos Rosas, 23, E-28003 Madrid, Spain.

[1] Sea surface temperature (SST), marine productivity, and fluvial input have been reconstructed for the last 11.5 calendar (cal) ka B.P. using a high-resolution study of C_{37} alkenones, coccolithophores, iron content, and higher plant *n*-alkanes and *n*-alkan-1-ols in sedimentary sequences from the inner shelf off the Tagus River Estuary in the Portuguese Margin. The SST record is marked by a continuous decrease from 19°C, at 10.5 and 7 ka, to 15°C at present. This trend is interrupted by a fall from 18°C during the Roman and Medieval Warm Periods to 16°C in the Little Ice Age. River input was very low in the early Holocene but increased in the last 3 cal ka B.P. in association with an intensification of agriculture and deforestation and possibly the onset of the North Atlantic Oscillation/Atlantic Multidecadal Oscillation modes of variability. River influence must have reinforced the marine cooling trend relative to the lower amplitude in similar latitude sites of the eastern Atlantic. The total concentration of alkenones reflects river-induced productivity, being low in the early Holocene but increasing as river input became more important. Rapid cooling, of 1–2°C occurring in 250 years, is observed at 11.1, 10.6, 8.2, 6.9, and 5.4 cal ka B.P. The estimated age of these events matches the ages of equivalent episodes common in the NE Atlantic–Mediterranean region. This synchronicity reveals a common widespread climate feature, which considering the twentieth century analog between colder SSTs and negative North Atlantic Oscillation (NAO), is likely to reflect periods of strong negative NAO.

Copyright 2009 by the American Geophysical Union

Components: 9648 words, 6 figures, 2 tables.

Keywords: sea surface temperature; productivity; fluvial input; Holocene; Portuguese margin; Tagus mud patch.

Index Terms: 1050 Geochemistry: Marine geochemistry (4835, 4845, 4850); 4954 Paleoceanography: Sea surface temperature; 0420 Biogeosciences: Biomolecular and chemical tracers.

Received 18 December 2008; **Revised** 11 May 2009; **Accepted** 19 May 2009; **Published** 23 July 2009.

Rodrigues, T., J. O. Grimalt, F. G. Abrantes, J. A. Flores, and S. M. Lebreiro (2009), Holocene interdependences of changes in sea surface temperature, productivity, and fluvial inputs in the Iberian continental shelf (Tagus mud patch), *Geochem. Geophys. Geosyst.*, *10*, Q07U06, doi:10.1029/2008GC002367.

Theme: Circum-Iberia Paleoceanography and Paleoclimate: What Do We Know?
Guest Editors: F. Abrantes, C. Ruehlemann, M. F. Sánchez-Goñi, and A. Voelker

1. Introduction

[2] Until recently the present interglacial, the Holocene, has been considered as a period of stable climate [*McManus et al.*, 1999]. However, high-resolution studies of paleoproxies in marine sediments [*Bianchi and McCave*, 1999; *Cacho et al.*, 2001; *Frigola et al.*, 2007] and ice cores [*O'Brien et al.*, 1995], as well as dust records [*Jackson et al.*, 2005], have revealed the occurrence of suborbital millennial-scale climate variability during the last 11 cal ka B.P. of the Holocene [*Bianchi and McCave*, 1999; *Bond et al.*, 1997, 2001; *Cacho et al.*, 2001; *Dokken and Jansen*, 1999; *Frigola et al.*, 2007; *Lorenz et al.*, 2006; *Sarnthein et al.*, 2003]. Since the early studies of the Holocene in the North Atlantic Ocean, the occurrence of a 1,500-year cycle has been attributed to solar activity [*Bond et al.*, 2001], to ocean current intensity variation [*Bianchi and McCave*, 1999], or yet to atmospheric processes linked to the North Atlantic Oscillation [*Giraudeau et al.*, 2000]. During this period, sea surface temperature (SST) reconstructed by the alkenone method shows long-term cooling in the northeast Atlantic (36°N to 75°N) and in the Mediterranean Sea, involving drops of 1.2–2.9°C between the Holocene Optimum and the present [*Marchal et al.*, 2002]. This temperature decrease is consistent with other climate proxy records and with model simulations based on Milankovitch forcing [*Lorenz et al.*, 2006; *Marchal et al.*, 2002]. At 10.2 cal ka B.P., a SST fall of 1–1.5°C marks the Preboreal oscillation in the North Atlantic, which in turn corresponds to a southward advance of the polar front by about 500 km [*Ruddiman and McIntyre*, 1981]. The most extreme cold episode of this present interglacial was the 8.2 cal ka B.P. "event" detected in North Atlantic marine deep sea sediments by several climate proxy data. This '8.2 event' is often attributed to a meltwater outflow from the Hudson Basin (Canada) deglaciation into the North Atlantic Ocean and the consequent slowdown of the North Atlantic Deep Water formation [*Alley et al.*, 1997; *Alley and Ágústsdóttir*, 2005; *Barber et al.*, 1999; *Clark et al.*, 2002; *Mayewski et al.*, 2004]. The introduction of large amounts of freshwater into the North Atlantic triggers an important decrease of SST that occurs earlier and lasts longer than the isotopic signal recorded in the Greenland ice cores [*Alley et al.*, 1997; *Clark et al.*, 2001; *Kleiven et al.*, 2008], as shown by long climate cooling anomalies of multicentennial scale between ~8.9 and 8 cal ka B.P. [*Ellison et al.*, 2006; *Naughton et al.*, 2007a; *Rohling and Pälike*, 2005].

[3] Climate changes identified during the late Holocene have been less severe like the Roman Period (RP, A.D. 0–400 [*Lamb*, 1985]), the Medieval Warm Period (MWP, A.D. 800–1300 [*Hughes and Diaz*, 1994]) and the subsequent Little Ice Age (LIA, A.D. 1350–1900 [*Bradley and Jones*, 1993]).

[4] All the above referred studies and many other available in the literature provide an oceanic perspective of such climate changes since they were performed in cores retrieved from open sea sites. The continental response, although also reconstructed from marine sediment cores [*Naughton et al.*, 2007b; *Roucoux et al.*, 2006; *Sánchez-Goñi et al.*, 2002], has been mainly studied in other paleoarchives such as ice cores [*O'Brien et al.*,

1995], lake sediments [*Cranwell*, 1973], speleothems [*Baldini et al.*, 2008] and tree rings [*Briffa et al.*, 2002]. Marine and continental approaches give complementary information, but the dependence of the respective climate reconstructions from different paleoarchives restricts the possibilities of an integrated understanding of the overall changes. The use of the same archive in interface areas between the ocean and the continent has a strong potential for providing a better combined picture of the climate processes than those emerging from separate studies. In this perspective, climate reconstructions have also been done from continental shelf sediments. Besides variations in SST or salinity (SSS), these environments also record major variations in discharge of continental materials that affect the areas under fluvial influence [*Amorosi et al.*, 2005; *Müller and Stein*, 2000; *Rivera et al.*, 2006; *Stein et al.*, 2004; *Tanabe et al.*, 2006; *Xiao et al.*, 2006] and experience significant coastline variations [*Lambeck and Chappell*, 2001; *Siddall et al.*, 2003, 2004, 2006; *Yokoyama et al.*, 2000].

[5] Studies of marine cores close to continental landmasses have been performed in sites such as the Arabian Sea (ODP Site 723A [*Gupta et al.*, 2003]), western tropical Atlantic (GeoB3129-3911 [*Weldeab et al.*, 2006]), eastern tropical Atlantic (GeoB 6518 [*Schefuß et al.*, 2005; *Weijers et al.*, 2007]), Gulf of Guinea (MD03-2707 [*Weldeab et al.*, 2007]), eastern equatorial Pacific Ocean (EEP [*Leduc et al.*, 2007]), Timor Sea (MD01-2378 [*Xu et al.*, 2006]) and Cap Blanc (ODP Site 658C [*deMenocal et al.*, 2000b]). Those sites are located at water depths of 807, 830, 962, 1295, 1619, 1738 and 2263 m, respectively, which is obviously deeper than the continental shelf. On the other hand, there is a large number of studies concerning the variability of sediment supply in different coastal areas, like the Laptev Sea [*Müller and Stein*, 2000; *Rivera et al.*, 2006], the Amazon Basin [*Maslin and Burns*, 2000], the Yangtze River [*Liu et al.*, 2004; *Xiao et al.*, 2006], the Kara Sea [*Stein et al.*, 2004], the Mahakam Delta [*Storms et al.*, 2005], the Po River [*Amorosi et al.*, 2005] or the Red River delta system [*Tanabe et al.*, 2006], but they lack the information from the climate proxies performed in open sea sites.

[6] Until now, few previous studies have considered both climate change and river contribution to the continental shelf during the late Holocene (e.g., the Tagus mud patch, water depths 88–96 m [*Abrantes et al.*, 2005; *Lebreiro et al.*, 2006]; the Muros Ria, water depths 33–38 m [*Diz et al.*, 2002; *Lebreiro et al.*, 2006]).

[7] The Tagus River crosses the Iberian Peninsula and discharges a major load of suspended organic-rich sediments into the continental shelf off Lisbon forming the Tagus mud patch [*Cabeçadas and Brogueira*, 1997; *Gaspar and Monteiro*, 1977; *Vale*, 1981; J. H. Monteiro and I. M. C. Moita, personal communication, 1971]. Variations in river contribution and seasonal changes in coastal hydrology are described for the Cape Roca upwelling filament area for the last 2 ka [*Abrantes and Moita*, 1999; *Abrantes et al.*, 2005; *Fiúza*, 1983; *Moita*, 2001]. Going further, the present work extends the initial evaluation of *Abrantes et al.* [2005] back to 11.5 ka. Biomarkers have been analyzed at high-resolution using the $U^{K'}_{37}$ index to determine SST. Primary productivity is estimated from the alkenone concentration and coccolithophore's assemblages and TOC, while river input is reconstructed from the concentration of Fe and higher plant *n*-alkanes and *n*-alkan-1-ols. The combined study of the these proxies contributes to understand the Holocene climate evolution in eastern Atlantic coastal areas providing unambiguously time-related information on changes occurring in the marine and continental environment and their interaction.

2. Material and Methods

[8] The study area is located in the western Portuguese continental shelf, between Cape Raso and Cape Espichel (Figure 1), in a region strongly influenced by the Tagus River. The Tagus is the longest river in the Iberian Peninsula. Periodic flood events lead to major discharge of suspended and bed load sediments [*Vale*, 1981]. The sediments transported in suspension are preferentially deposited at the inner and middle shelf, and are characterized by organic-rich silty clays (>80%) [*Gaspar and Monteiro*, 1977; Monteiro and Moita, personal communication, 1971].

[9] Two sedimentary sequences are studied in this paper: a composite of box core PO287-26B, gravity core PO287-26G and piston cores D13902; and the piston core D13882 (Table 1 and Figure 1). The box core and the gravity core were retrieved in May 2002 during the PALEO 1 campaign on board the RV POSEIDON [*Monteiro et al.*, 2002]. The piston cores were collected during the Discovery cruise 249 in August–September 2000 using the National Oceanography Centre long-piston coring system (Table 1). The first 189 cm of core D13902

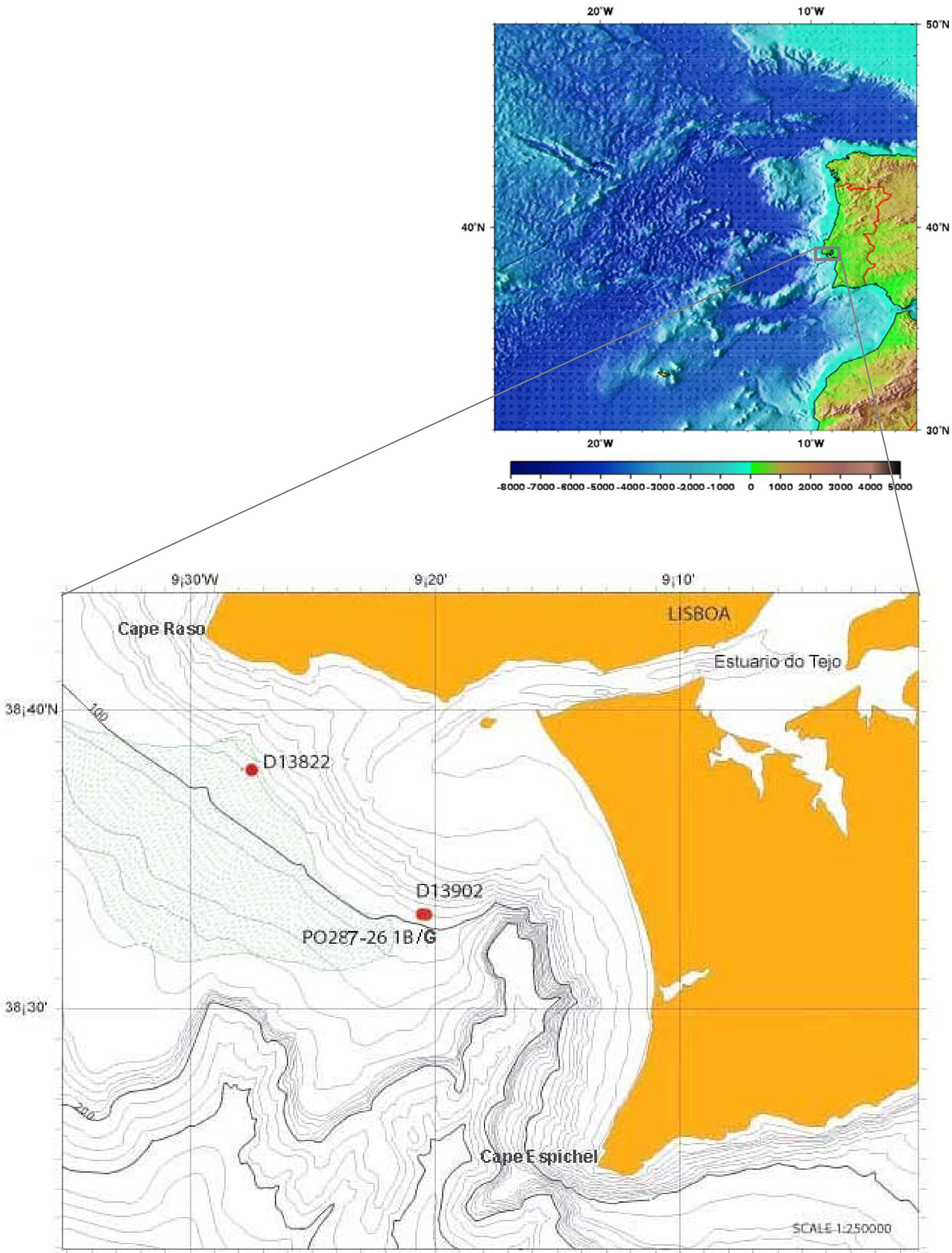

Figure 1. Area of study indicating the position of the sedimentary sequences used in this work.

Table 1. Location, Water Depth, and Length of the Studied Cores

Core ID	Core Type	Water Depth (m)	Core Length (m)	Latitude (N)	Longitude (W)
PO287-26-B	box	96	0.32	38°33.49′	9°21.84′
PO287-26-G	gravity	96	3.05	38°33.49′	9°21.84′
D13902	piston	90	6.00	38°33.24′	9°20.13′
D13882	piston	88	13.61	38°38.07′	9°27.25′

were disturbed and half-filled. As age determinations confirmed this disturbance, the zero depth of the core was moved downward to the 189 cm liner level [*Abrantes et al.*, 2005].

[10] Iron (Fe) concentrations in counts per 30 s (cts) were determined at 1 cm intervals in cores PO287-26 and D13882 and at 2cm intervals in core D13902 by X-ray fluorescence core scanning for nondestructive semiquantitative analysis of major elements [*Jansen et al.*, 1998] at Bremen University.

[11] For biomarkers analyses and TOC measurements, sediments were sampled every 1 cm in the box core, every 2–5 cm in cores D13902 and PO 287-26G, and every 5 cm in piston core D13882.

[12] Haphtophyte-synthesized C_{37} alkenones and higher-plant biomarkers, such as C_{23}-C_{33}*n*-alkanes and *n*-alkan-1-ols C_{20}-C_{30}, were analyzed following the methods described by *Villanueva et al.* [1997]. Briefly, sediment samples (2 g) were freeze-dried and extracted by sonication with dichloromethane and then hydrolyzed with 6% potassium hydroxide in methanol. After derivatization with bis(trimethylsilyl)trifluoroacetamide, the extracts were analyzed with a Varian gas chromatograph Model 3400 equipped with a septum programmable injector and a flame ionization detector. The concentrations of each compound were determined using nonadecan-1-ol, hexatriacontane and tetracontane as internal standards.

[13] Selected samples were analyzed by gas chromatography coupled to mass spectrometry (GC-MS) for compound verification and identification of possible coelutions. The GC-MS used was a Fisons MD800 (THERMO Instruments, Manchester, UK). The carrier gas was helium (flow 2.1 mL/min). Injection and transfer line temperatures were 300°C. The quadrupole mass spectrometer was operated in EI mode (70 eV), scanning between *m/z* 50–650 in 1 s. The ion source temperature was 200°C.

[14] SST determinations were based on the alkenone unsaturation index, $U^{K'}_{37}$, which was calibrated to the temperature equation of *Müller et al.* [1998]. Replicate injections and sample dilution tests allowed assessing measurement errors to less than 0.5°C [*Grimalt et al.*, 2001].

[15] Total organic and inorganic carbon was determined on aliquots (2 mg) of dry and homogenized sediment subsamples of the same levels used for biomarker determination. Total carbon was analyzed in the ground sediment with a CHNS-932 Leco elemental analyzer. Aliquots of those same samples were burnt at 400°C in an oven and further analyzed for determination of the inorganic carbon weight %. Organic carbon (OC) weight % was calculated by difference between the two measurements. The relative precision of repeated measurements of both samples and standards was 0.03 wt%.

[16] Smear slides for coccolithophore identification were prepared as described by *Flores and Sierro* [1997]. A light polarizing microscope (1250x) was used for observation and counting.

3. Chronology

[17] The age models are based on 18 accelerator mass spectrometry (AMS) ^{14}C dates of *Turritela* and other mollusk shells and 16 ^{210}Pb measurements in the top part of the sequence. These ^{14}C dated samples were chosen from core D13882 (six), core D13902 (eight) and core PO287-26G (three) and one in the bottom of box core PO287-26B (Table 2). All samples were collected at levels with no evidence of reworking, that is, the shells selected were the ones found in their living position, well integrated in the sediment level and in good degree of preservation. When available, complete bivalve mollusks still articulated were selected.

[18] The age model for the last 2 cal ka B.P. of cores D13902 and PO287-26B/G is reported by *Abrantes et al.* [2005]. The top part of core D13882 was correlated to D13902 via the Fe and MS records (Table 2 and Figure 2). Furthermore, six AMS-^{14}C dates from core D13882 and one from D13902, using the MARINE04 calibration data and CALIB 5.0 program, were used for the rest of the sequence [*Hughen et al.*, 2004; *Stuiver and Reimer*, 1993; *Stuiver et al.*, 1998]. As such, all ages listed through the rest of the text correspond to calendar ka (ka = 1000 years) B.P. but will be referred as ka for simplification.

Table 2. Results of AMS Dating of the Tagus Mud Patch, Box, Gravity, and Piston Cores

Lab Code	Sample ID	Spliced/Corrected Depth[a] (cm)	Sample Type	^{14}C Age (B.P.)	Calendar Age (B.P.)	Error	Age (A.D.)
AAR-8368.2[b]	PO287-26B	51	mollusk shell	440	51	25	1899
OS-42380[b]	PO287-26G	21	mollusk shell	55	>1950		
OS-42381[b]	PO287-26G	86	mollusk shell	545	186	25	1764
KIA 23661[b]	PO287-26G	125	mollusk shell	905	855	25	1095
AAR-7825[b]	D13902 (27–28)	75.4	mollusk shell	492	111	39	1839
AAR-7207[b]	D13902 (62–63)	110.4	mollusk shell	1160	691	45	1259
AAR-7208[b]	D13902 (62–63)	110.4	turritela	1185	704	40	1246
AAR-7209[b]	D13902 (96–97)	144.4	mollusk shell	1370	863	45	1087
OS-37307[b]	D13902 (124–125)	172.4	foraminifera	1880	1394	160	556
AAR-7828[b]	D13902 (151–152)	199.4	mollusk shell	2007	1487	37	463
AAR-7210[b]	D13902 (199–200)	247.4	mollusk shell	2340	1885	55	65
OS-37710	D13902 (342–343)	390.4	mollusk shell	5860	6270	40	
OS- 37706	D13882	257	turritela	1960	1511	45	
KIA 27301	D13882	464	turritela	2920	2710	35	
KIA 29730	D13882	522	mollusk shell	3690	3596	30	
KIA 27303	D13882	632	turritela	6120	6542	55	
KIA 29729	D13882	699	mollusk shell	8215	8753	45	
KIA 29728	D13882	738	mollusk shell	9735	10614	55	

[a] Spliced for core D13902.
[b] Data published by *Abrantes et al.* [2005].

[19] The age model of box core PO287-26B, elaborated from the ^{210}Pb measurements and using the values determined in two levels collected from D13902 as background level, result in a sedimentation rate of 0.47 cm a^{-1} and a temporal resolution of 2 years per centimeter. The same resolution was found in the upper 75 cm of piston core D13902 and the top 100 cm of gravity core PO287-26G.

[20] In cores D13902 and PO287-26G sedimentation rates were 0.11 and 0.14 cm a^{-1}, allowing resolutions of 9 and 7 years, respectively [*Abrantes et al.*, 2005]. In core D13902, the section between 95 cm and 76 cm showed an instantaneous deposit of reworked material as consequence of the Lisbon earthquake and its associated tsunami [*Abrantes et al.*, 2005]. Considering the last dated level below this event and the year of this earthquake (A.D. 1755) it was assumed that 355 years of record were eroded. The same event was found in core PO287-26G where approximately 160 years of the core were lost. For core D13882, sedimentation rates vary between 0.02 cm a^{-1} and 0.2 cm a^{-1} allowing a temporal resolution between 4 and 48 years, respectively.

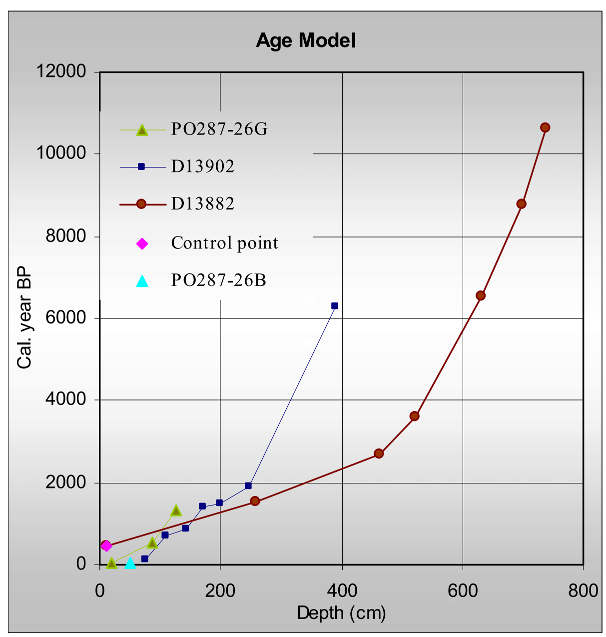

Figure 2. Age models between 0 and 10 500 cal A.D. for cores D13882, D13902, and PO287 26G and B based on accelerator mass spectrometry ^{14}C dating of marine carbonates. The top age for the core D13882 was defined on the basis of a correlation with the top part of D13902. The age model for the last 2000 years B.P. (cores D13902 and PO287 26G/B) was published by *Abrantes et al.* [2005].

4. Results

4.1. Sea Surface Temperature

[21] The $U_{37}^{K'}$-SST record of the composite Holocene sediment sequences (Figure 3a) fluctuates

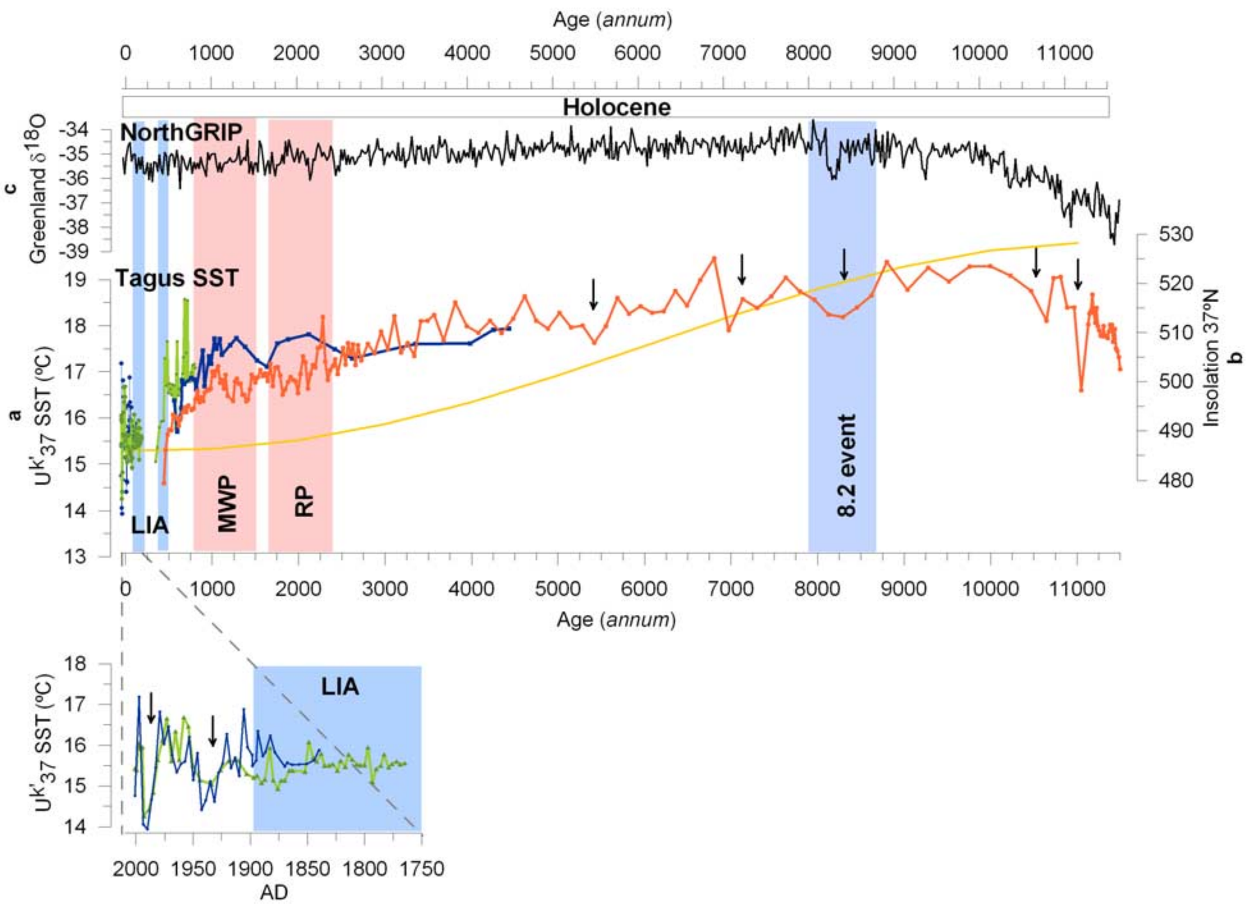

Figure 3. (a) $U^{K'}_{37}$-SST profile along the Tagus mud patch sequences for the last 11 ka. (b) The 21 June insolation curve at 37°N. (c) Greenland δ^{18}O record from NGRIP [*Johnsen et al.*, 2001; *North Greenland Ice Core Project Members*, 2004; *Rasmussen et al.*, 2006]. The vertical arrows show cooling events in the Holocene. Note that in the x scale there is a change in time amplitude before and after year 2000 B.P. RP, Roman Period; MWP, Medieval Warm Period; LIA, Little Ice Age.

between 19°C and 14°C, showing maximum values between 11–6 ka and a minimum at the beginning of the 1990s. Furthermore, it exhibits a 4°C-decreasing trend between 10 ka and the present but is interrupted between 2 and 0.6 ka by the RP and the MWP. At the end of the MWP, there is an additional 2°C cooling, to an average temperature of 15.5°C, marking the beginning of the LIA. The last 130 years exhibit a strong variability with marked minima at A.D. 1930–1940 and A.D. 1990, 14.5°C and 14°C, respectively, and maxima of about 17°C at A.D. 1905, A.D. 1950–1970 and A.D. 1995. These changes involve SST drops and increases of 3°C in periods of 10 years or less (Figure 3a).

4.2. Paleoproductivity

[22] Total alkenones have been used as paleoproductivity indicators in open ocean sites [*Schubert et al.*, 1998; *Schulte et al.*, 1999; *Villanueva et al.*, 1998; *Villanueva et al.*, 2001]. In coastal areas, rivers input both particles and nutrients. While the particles will dilute the flux of sediments relative to the alkenone carrying organisms, the nutrients may enhance algal productivity. Off the Tagus, coccolithophores are dominant most of the year [*Moita*, 2001], governing the phytoplankton composition during winter and early spring when influence of nutrients from the river is high. Only during the upwelling season (May to September) are these algae outcompeted by diatoms [*Abrantes and Moita*, 1999]. On this basis alkenones may not be good markers for upwelling related productivity.

[23] In our sediments, the concentration of total alkenones is low (200 ng/g, or less than 20 ng/cm^2/a^1) during the early Holocene, starting to rise at 5.5 ka and becoming more pronounced (up to 800 ng/g, or 300 ng/cm^2/a^1; Figures 4b and 4c) after 3 ka.

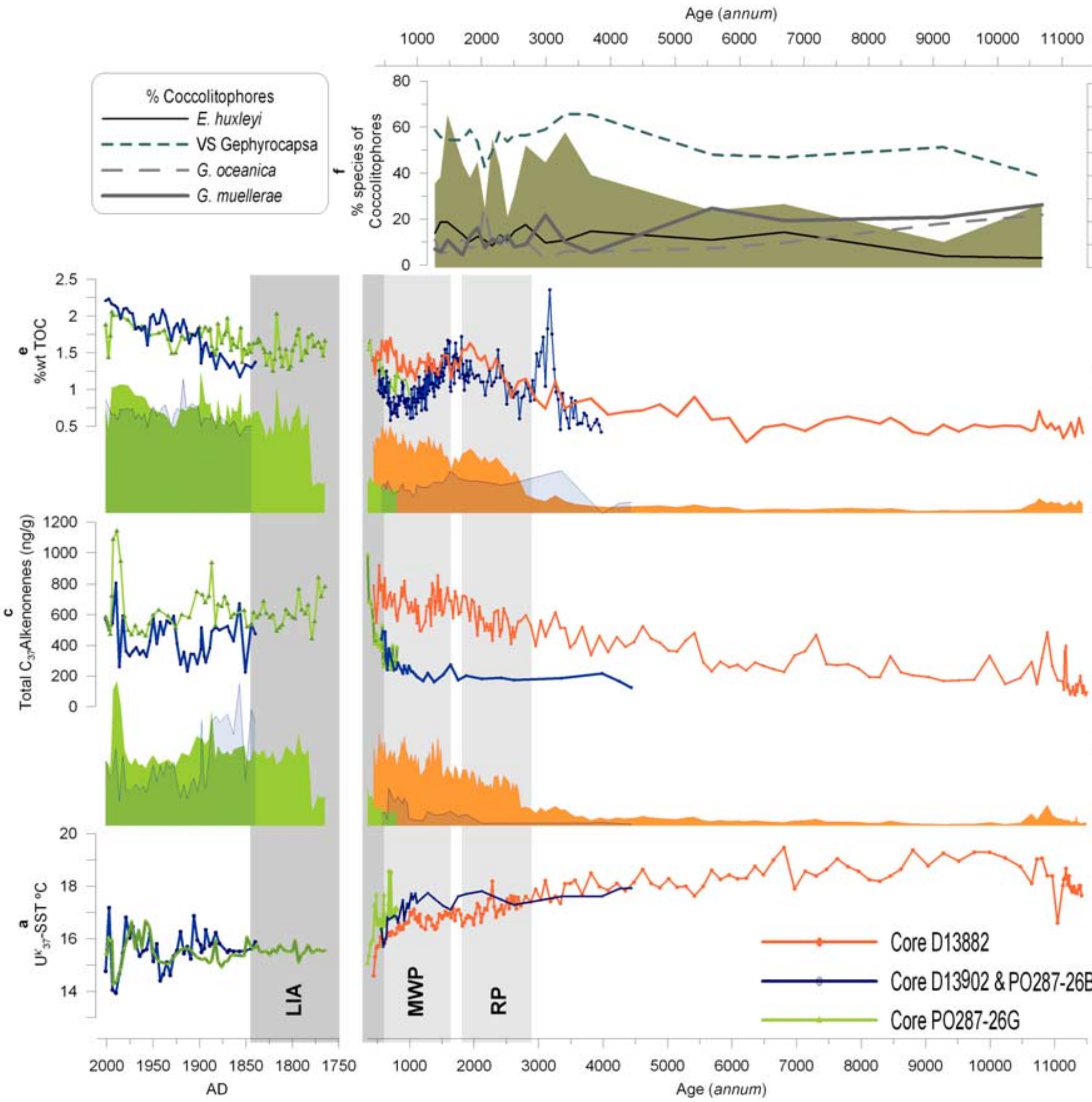

Figure 4. Productivity proxies along the sedimentary sequences. (a) SST-$U^{K'}_{37}$. (b) Flux of total C_{37} alkenones. (c) Concentration of C_{37} alkenones (ng/g). (d) Flux of total organic carbon. (e) Total organic carbon (%wt). (f) Percentage of coccolithophore species and (g) flux of total coccolithophores (ng/cm^2/a). RP, MWP, and LIA as in Figure 3.

This same trend is observed for the total organic carbon (TOC) that ranges between 0.3 and 2% (Figure 4e). The strong similarity between these two proxies in D13882 supports a response to high amounts of river-transported nutrients to the coastal area, in particular during the last 3 ka.

[24] Examination of the distribution of coccolithophores reveals *Gephyrocapsa* (*G.*) as the most abundant genus, with dominance of the small sized *Gephyrocapsa* (<3 μm) followed by *G. oceanica* and *G. muellerae* (Figure 4f). While the group of small *Gephyrocapsa* and *G. oceanica* is known to live in nutrient rich environments [*Brand*, 1994; *Wells and Okada*, 1997; *Winter et al.*, 1994], *G. muellerae* is characteristic of cold waters [*Flores and Sierro*, 1997].

4.3. River Contribution

[25] The influence of the Tagus River discharge in the studied area is easily observed in the satellite and space shuttle images [*Abrantes et al.*, 2005]. C_{23}-C_{33}*n*-alkanes and C_{20}-C_{30}*n*-alkan-1-ols originate from higher plants [*Eglinton and Hamilton*, 1967] and their concentrations in the continental shelf can be used as an indicator for fluvial terrigenous input [*Grimalt et al.*, 1990]. In addi-

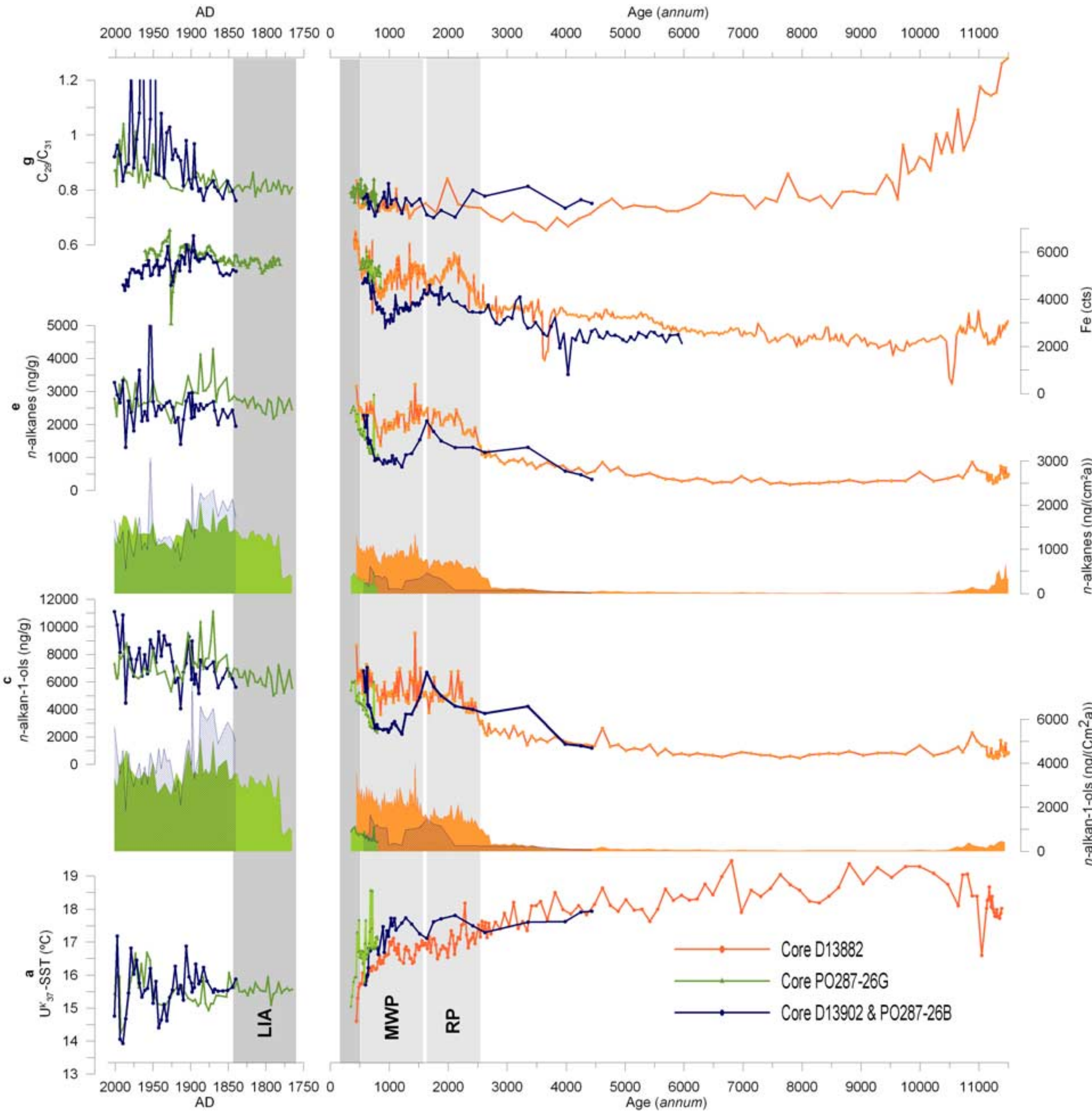

Figure 5. Terrigenous inputs along the sedimentary sequences. (a) SST-$U^{K'}_{37}$. (b) Flux of *n*-alkan-1-ols (ng/cm^2/a). (c) Concentrations of *n*-alkan-1-ols (ng/g). (d) Flux of *n*-alkanes (ng/cm^2/a). (e) Concentrations of *n*-alkanes (ng/g). (f) Fe content determined by XRF (cts units). (g) Ratio between C_{29} and C_{31} *n*-alkanes. RP, MWP, and LIA as in Figure 3.

tion, changes in the concentration of lipid compounds give information on the type of continental vegetation close to the study area. The alkanes index (C_{29}/C_{31}) has been defined on the basis of the existing relationship between the two main *n*-alkanes compounds following the suggestions made by previous studies [*Cranwell*, 1973; *Poynter and Eglinton*, 1990; *Tareq et al.*, 2005]. This index allows us to know about the kind of vegetation that dominates in the river's hydrographic basin, in the adjacent continent. An index <1 reflects higher abundance of the alkane with 31 carbon atoms and indicates the dominance of grass and herbaceous plants. An index >1 results from a larger amount of alkanes with 29 carbon atoms, and so, the dominance of trees and shrubs in the adjacent continent.

[26] These Tagus sequences show a clear prevalence of C_{29} during the early Holocene (Figure 5g). The concentrations of *n*-alkane-1-ols (Figure 5c)

are currently higher (up to 11,000 ng/g) than those of *n*-alkanes (up to 4,000 ng/g, Figure 5e). However, both terrigenous proxies exhibit a similar trend, pointing to a common origin. The concentrations of these biomarkers are also parallel to the Fe content as measured by XRF (Figure 5f). This metal is a good marker for terrigenous input and therefore for river contribution. These three markers together validate clear trend toward higher terrigenous input in the last 3 ka, coincident with the onset of Neoglaciation [*Andersson et al.*, 2003; *Bauch and Weinelt*, 1997].

5. Discussion

5.1. Climate Variability and River Evolution During the Holocene

[27] The continuous SST decreasing trend observed between 10.5–7 ka and the present (Figure 3a) follows the summer insolation at 37°N (Figure 3b). Similar trends have also been detected in $U^{K'}_{37}$-SST records from extratropical sites of the Atlantic Ocean (between −0.69 and +4.41°C [*Marchal et al.*, 2002]), contrary to the warming progress observed in the Pacific Ocean (between −0.31 and +1.08°C [*Kim et al.*, 2004]) and in tropical areas (between +0.19 and +1.05°C [*Lorenz et al.*, 2006]). This divergent SST evolution in the Atlantic and the Pacific is attributed to a dipole pattern generated by the interaction between the positive Pacific North American Oscillation (PNA) and the negative North Atlantic Oscillation (NAO) phases by *Kim et al.* [2004], while *Lorenz et al.* [2006] attribute the divergent Holocene climate trend between northern and tropical locations to seasonally opposing insolation changes.

[28] The strong cooling of 4°C observed in the Tagus record is of similar intensity to that found at high latitudes, such as the North Atlantic [*Marchal et al.*, 2002], but differs from the cooling trends of lower intensity observed in other similar latitudes sites [*Cacho et al.*, 2001; *Marchal et al.*, 2002]. This strong SST decrease may reflect higher sensitivity to seasonal changes by continental influence, e.g., an additional cooling effect due to the fact that in the cold seasons, river waters are cooler than seawater. An influence reflected by a clear contrast between river and sea surface temperature, recognized in satellite images (Figure 6) (P. Oliveira et al., personal communication, 2007). As such, the river output of colder waters resulted in a relatively stronger Holocene SST cooling gradient in this area. A gradient that is also noticeable in the terrigenous markers which show a continuous increase toward the Late Holocene (Figures 5b–5f).

[29] The period between 10 and 8 ka, reflects the highest sea surface temperatures of the Holocene in the western Iberian margin, and is also marked by the maximum extent of forested area, with the predominance of pine forests along the Portuguese coast [*Queiroz*, 1999], oak in high altitudes, like in the Serra da Estrela mountains [*Van der Knaap and Van Leeuwen*, 1985] and by oak and pine in the midaltitude and low-altitude sites of the northwestern Iberian Peninsula [*Naughton et al.*, 2007b]. This suggests that both the Iberian margin and the adjacent landmasses have experienced the highest sea and atmospheric temperature values at the beginning of the Holocene. The C_{29}/C_{31} ratio shows a remarkable coincidence with the abundance of semidesert plants [*Naughton et al.*, 2007b; *Turon et al.*, 2003]. In the Early Holocene, the C_{29} is dominant and the alkane index is higher than 1 indicating forest cover with high soil stability and consequently, lower drainage. From 9 to 6 ka the concentration of terrigenous markers and Fe content is continuously low, accompanying the SST decrease, and in good agreement with the gradual contraction of the forest defended by *Naughton et al.* [2007b] and *Turon et al.* [2003].

[30] In terms of sea level, at ^{14}C 10 ka the regional curve of *Dias et al.* [2000] indicates a sea level 60 m below its present level, resulting in a water depth of 40 m at the study area. On the lower Tagus valley, river sediments of that age correspond to channel deposits [*Vis et al.*, 2008], and is only after 9 ka that the retention of sediments inside the estuary becomes important. A retention that caused a major decrease in the amount of terrigenous material transported to the deep sea through the Lisbon canyon (F. Abrantes et al., Sedimentation processes on the Tagus river system (Portuguese Margin) during the Holocene—SEDPORT main results, paper presented at European Geosciences Union General Assembly, Vienna, 1–7 April 2006), and possibly also to the shelf, although not reflected in the sedimentation rate (SR) (Figure 2).

[31] Between 6 and 3 ka, changes in the vegetation patterns on land are associated with deforestation. Soils became unstable and contribute more to river input. Concentrations of *n*-alkanes and *n*-alkan-1-ols start to rise progressively at 6 ka to a rapid increase around 3 ka, apparently coincident with the onset of the Atlantic Mutidecadal Oscillation (AMO) mode of variability [*Lorenz et al.*, 2006]. High concentrations are maintained up to the present.

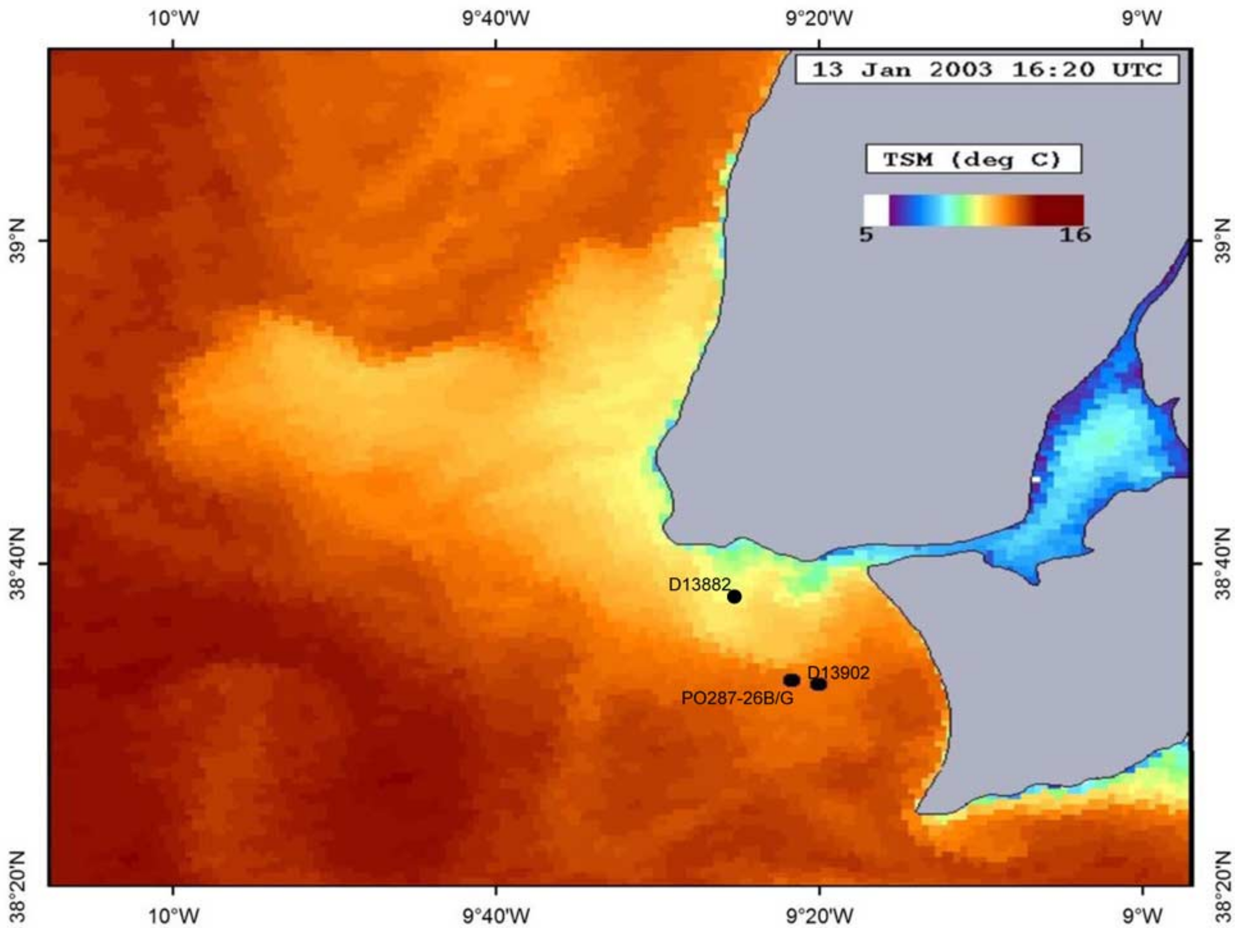

Figure 6. Satellite images of the river water sea surface temperature on Tagus mud patch. Projection data: Geographic Coordinate System. Datum: WGS_1984 (Oliveira et al., personal communication, 2007). Figure courtesy of Oceanography Spatial Center, Oceanography Institute of Portugal.

Compared to the Holocene Climatic Optimum, during the two last warm periods, the Roman and the Medieval Warm Periods, the terrigenous biomarkers show prominent concentrations along with higher Fe contents. These enrichments are not coincident with SST drops. In fact, between 3 and 1.5 ka, pollen records from the southern Tagus River basin confirm an increase in agriculture activity and suggest deforestation and possibly higher soil erosion [*Mateus*, 1992; *Queiroz*, 1999]. Therefore, a higher concentration of terrigenous biomarkers during these warm periods seems a more direct response to an increase in soil use at times of amerioration than to river flow enhancement and climate cooling or high sea level stands.

5.2. Short-Term Variability

[32] Short cooling episodes of 1–2°C punctuate the general SST cooling trend at 11.1, 10.6, 8.2, 6.9 and 5.4 ka (Figure 3a). Within dating errors these episodes exhibit a very good match with the millennial-scale variation observed during the Holocene both in high- and low-latitude sites like in the North Atlantic (11.1, 10.3, 8.2 and 5.9 ka [*Bond et al.*, 1997]), the Alboran Sea (11.0, 10.3, 8.2 and 5.4 ka [*Cacho et al.*, 1999]), the Thyrrenian Sea (11.6, 9.9, 5.9 ka [*Cacho et al.*, 2002]), the Gulf of Cadiz (10 and 8.0 ka [*Cacho et al.*, 2000]), and in subtropical west Africa ODP Site 658C (10.2, 8.0, 6.0, 4.6, 3.0, 1.9 ka [*deMenocal et al.*, 2000b]). These cooling episodes are therefore not just a local effect and must represent a recurrent climatic instability in the northeast Atlantic-Mediterranean region at least, which considering the twentieth century positive relationship between colder SSTs and NAO negative modes as an analog, are likely to reflect periods of strong negative NAO.

[33] In the Tagus mud patch the longest and better marked of these cooling episodes is the 8.2 ka

cooling that lasted about 700 years. This event was the most intense cooling recorded in the GISP 2 [*Alley et al.*, 1997] and NGRIP Holocene records (Figure 3b) [*Johnsen et al.*, 2001; *North Greenland Ice Core Project Members*, 2004; *Rasmussen et al.*, 2006]. Several studies show similar amplitude of duration for this event. In northwestern France the maximum expansion in *Corylus* woodlands (between circa 8.74 and 8.06 ka) was associated with a high seasonality episode [*Naughton et al.*, 2007a], and occurs synchronously with a succession of events that starts with the last stages of the Laurentide Ice sheet decay and the catastrophic final drainage episodes of the "glacial lakes Agassiz-Ojibway" into the Hudson Bay at around 8.470 ka [*Clarke et al.*, 2004] (error range of 8.160–8.740 ka [*Barber et al.*, 1999]), followed by the consequent 8.2 ka event [*Clarke et al.*, 2004; *Teller et al.*, 2002]. The introduction of large amounts of freshwater into the North Atlantic triggers the decrease in sea surface temperatures, and earlier start than the 8.2 ka isotopic event of the Greenland ice cores, lasting several centuries, between ~8.9 and 8 ka [*Ellison et al.*, 2006]. This multicentennial SST cooling detected in the high-resolution North Atlantic deep-sea core MD99-2251 is roughly contemporaneous of the climate cooling defined by *Rohling and Pälike* [2005], and has also been observed between ~8.6 and 8 ka in other regions of the North Atlantic, such as the Laurentian Fan and the north of Iceland [*Keigwin et al.*, 2005; *Knudsen et al.*, 2004].

[34] In the last 1.5 ka the Tagus mud patch SST record shows higher amplitude of decadal to subdecadal variation (Figure 3a). The warm phase between 1.3 and 0.75 ka (SST ~ 17°C) is coincident with the MWP [*Cronin et al.*, 2003; *Dahl-Jensen et al.*, 1998; *deMenocal et al.*, 2000a; *Jones et al.*, 2001; *Jones and Mann*, 2004]. The available sedimentary record for the beginning of the LIA [*deMenocal et al.*, 2000a; *Jones et al.*, 2001; *Jones and Mann*, 2004; *Keigwin*, 1996] (0.18 to 0.08 ka; Figure 3), exhibits a rapid decrease to SST values 2°C lower than those of the MWP. However, when looked in detail while both the RP and the MWP are marked by an increase in SST at site D13902 accompanied by a decrease in Fe, site D13882 shows a slight decreasing tendency in SST. According to *Abrantes et al.* [2005], the RP and MWP were times of low river input but high marine production associated with strong coastal upwelling; this process is responsible for the SST decrease SST at site D13882. During cold periods, at our location, there is a general correspondence between the SST decrease (Figure 3a) and increase of river input (Figures 5b–5f) as reflected by higher concentrations of biomarkers of terrestrial origin and Fe. However, there are episodes of higher concentrations of terrigenous biomarkers that do not parallel the SST drops. These probably reflect changes in vegetation sources like those recorded in the C_{29}/C_{31} ratio (Figure 5g).

[35] Two rapid cooling periods are observed in the twentieth century, one between A.D. 1925–1950 involving a 2°C decrease, and another one, exhibiting a 3°C drop, extending from A.D. 1980 to A.D. 1990 (Figure 3a). These SST changes, namely the 3°C increase from 14 to 17°C, occurred within 3 years and is observed at A.D. 1994 in the instrumental record (F. Abrantes et al., Proxy calibration to Instrumental Data Set, paper presented at First MedCLIVAR Workshop on Reconstruction of Past Mediterranean Climate, Carmona, Spain, 2006). They follow variations from extreme positive to extreme negative values of the NAO index [*Houghton et al.*, 2001; *Jones and Mann*, 2004]. Although their larger amplitude of variation relative to older events might be valid, amplification may also result from the less severe smoothing effect generated by the compaction and bioturbation that generally occurs down core.

[36] The C_{37} alkenone productivity record shows concomitant changes with SST but in the opposite direction (Figure 4c) indicating higher alkenone production during cold episodes when higher amounts of continental material reflect increased river flow and nutrient incorporation into the marine environment (Figures 5b and 5e). These oscillations are likely to reflect NAO cyclicity [*Jones et al.*, 2001; *Trigo et al.*, 2002], since during negative phases the weak north-south pressure gradient induces storminess and precipitation in Southern Europe, leading to high precipitation anomaly fields in the Tagus Basin area during the winter months [*Trigo and DaCamara*, 2000]. Assuming that this mechanism has been operative during most of, or the entire Holocene [*Lorenz et al.*, 2006], it can be hypothesized that higher precipitation during negative NAO mode involved higher nutrients transport and therefore higher river-induced productivity at lower SST conditions.

6. Conclusions

[37] This high-resolution study of sedimentary sequences covering the last 11.5 ka provides the

first integrated picture of the marine and continental climate changes at the inner to middle Portuguese continental shelf site under the influence of the Tagus River. The obtained proxy data reveals climatic events comparable with existing open sea and inland sites, and help to clarify the land-sea interaction during the Holocene.

[38] The general decrease trend in Holocene SST, from 19°C at 11–7.0 ka to 15°C at present, follows the general summer insolation trend and is in agreement with observations in other midlatitude marine sites. However, the Tagus mud patch sequences exhibits higher amplitude of variation, involving a 4°C decrease, likely to reflect a continental climate-dependent influence besides the marine variability at the site. Furthermore, the higher amounts of terrigenous markers at lower SST suggest a land effect by means of colder river outflow.

[39] The occurrence of rapid cooling periods of 1–2°C within 250 years at 11.1, 10.6, 8.2, 6.9 and 5.4 ka, within the general Holocene SST decreasing trend, match the ages of similar events recorded in the NE Atlantic–Mediterranean area showing that they correspond to a common widespread climate feature. Higher-amplitude SST variation observed during the last 1.5 ka, relative to the preceding Holocene times, exhibit the warm Roman Period and MWP followed by a 2°C decrease during the LIA.

[40] Decadal to subdecadal cold episodes are also recorded in the twentieth century, e.g., a 2°C decrease at A.D. 1925–1950 and a 3°C drop at A.D. 1980–1990. These proxy-defined episodes are coincident with low instrumental values measured during NAO negative phases and suggest that the known climate sensitivity of the Tagus marine area to this index is superbly recorded in the sediments deposited during the 150 years of instrumental record.

[41] River influence is observed to increase toward recent times, when comparing the early with the later Holocene, including the RP and MWP, and might reveal that AMO variability has operated since 5–3 ka. This change goes together with the climate cooling observed in the SST records but may also reflect deforestation by agricultural activities. Higher river influence results in an increase in the amount of nutrients brought from the continent to the sea, and consequently higher river-induced marine productivity.

Acknowledgments

[42] Financial support was received from FCT (Fundação para a Ciência e Tecnologia) (SFRH/BD/13749/2003), EU projects SEDPORT (PDCTM/40017/2003) and HOLSMEER (EVK2-CT-2000-00060), the Spanish Ministry of Science and Technology (REN2003-08642-C02-01), Consolider-Ingenio 2100 Project CE-CSD2007-0067, and INETInovação. XRF measurements were made at University of Bremen through funding from the PaleoStudies program. We are grateful to C. Monteiro (INETI) for TOC measurements, R. Mas (IDAEA) for laboratory assistance, and Belén Martrat for useful comments.

References

Abrantes, F., and M. T. Moita (1999), Water column and recent sediment data on diatoms and coccolithophorids, off Portugal, confirm sediment record of upwelling events, *Oceanol. Acta*, *22*, 319333, doi:10.1016/S0399-1784(99)80055-3.

Abrantes, F., S. Lebreiro, T. Rodrigues, I. Gil, H. Bartels-Jonsdottir, P. Oliveira, C. Kissel, and J. O. Grimalt (2005), Shallow-marine sediment cores record climate variability and earthquake activity off Lisbon (Portugal) for the last 2000 years, *Quat. Sci. Rev.*, *24*, 2477–2494, doi:10.1016/j.quascirev.2004.04.009.

Alley, R. B., and A. M. Ágústsdóttir (2005), The 8k event: Cause and consequences of a major Holocene abrupt climate change, *Quat. Sci. Rev.*, *24*, 1123–1149, doi:10.1016/j.quascirev.2004.12.004.

Alley, R. B., P. A. Mayewski, T. Sowers, M. Stuiver, K. C. Taylor, and P. U. Clark (1997), Holocene climatic instability: A prominent, widespread event 8200 yr ago, *Geology*, *25*, 483–486, doi:10.1130/0091-7613(1997)025<0483:HCIAPW>2.3.CO;2.

Amorosi, A., M. C. Centineo, M. L. Colalongo, and F. Fiorini (2005), Millennial-scale depositional cycles from the Holocene of the Po Plain, Italy, *Mar. Geol.*, *222–223*, 7–18, doi:10.1016/j.margeo.2005.06.041.

Andersson, C., B. Risebrobakken, E. Jansen, and S. O. Dahl (2003), Late Holocene surface ocean conditions of the Norwegian Sea (Vøring Plateau), *Paleoceanography*, *18*(2), 1044, doi:10.1029/2001PA000654.

Baldini, L. M., F. McDermott, A. M. Foley, and J. U. L. Baldini (2008), Spatial variability in the European winter precipitation δ^{18}O-NAO relationship: Implications for reconstructing NAO-mode climate variability in the Holocene, *Geophys. Res. Lett.*, *35*, L04709, doi:10.1029/2007GL032027.

Barber, D. C., et al. (1999), Forcing of the cold event of 8,200 years ago by catactrophic drainage of Laurentide lakes, *Nature*, *400*, 344–348, doi:10.1038/22504.

Bauch, H. A., and M. S. Weinelt (1997), Surface water changes in the Norwegian Sea during last deglacial and Holocene times, *Quat. Sci. Rev.*, *16*, 1115–1124, doi:10.1016/S0277-3791(96)00075-3.

Bianchi, G. G., and I. N. McCave (1999), Holocene periodicity in North Atlantic climate and deep-ocean flow south of Iceland, *Nature*, *397*, 515–517, doi:10.1038/17362.

Bond, G., W. Showers, M. Cheseby, R. Lotti, P. Almasi, P. deMenocal, P. Priore, H. Cullen, I. Hajdas, and G. Bonani (1997), A pervasive millennial-scale cycle in North Atlantic

Holocene and glacial climates, *Science*, *278*, 1257–1266, doi:10.1126/science.278.5341.1257.

Bond, G., B. Kromer, J. Beer, R. Muscheler, M. N. Evans, W. Showers, S. Holffmann, R. Lotti-Bond, I. Hajdas, and G. Bonani (2001), Persistent solar influence on North Atlantic climate during the Holocene, *Science*, *294*, 2130–2136, doi:10.1126/science.1065680.

Bradley, R. S., and P. D. Jones (1993), Little Ice Age summer temperature variations: Their nature and relevance to recent global warming trends, *Holocene*, *3*, 367–376, doi:10.1177/095968369300300409.

Brand, L. E. (1994), Physiological ecology of marine coccolithophores, in *Coccolithophores*, edited by A. Winter and W. G. Siesser, pp. 39–49, Cambridge Univ. Press, Cambridge, U. K.

Briffa, K. R., T. J. Osborn, F. H. Schweingruber, P. D. Jones, S. G. Shiyatov, and E. A. Vaganov (2002), Tree-ring width and density data around the Northern Hemisphere: Part 1, Local and regional climate signals, *Holocene*, *12*, 737–757, doi:10.1191/0959683602hl587rp.

Cabeçadas, G., and M. J. Brogueira (1997), Sediments in a Portuguese coastal area—Pool sizes of mobile and immobile forms of nitrogen and phosphorus, *Mar. Freshwater Res.*, *48*, 559–563, doi:10.1071/MF96053.

Cacho, I., J. O. Grimalt, C. Pelejero, M. Canals, F. J. Sierro, J. A. Flores, and N. Shackleton (1999), Dansgaard-Oeschger and Heinrich event imprints in Alboran Sea paleotemperatures, *Paleoceanography*, *14*, 698–705, doi:10.1029/1999PA900044.

Cacho, I., J. O. Grimalt, F. Sierro, N. J. Shackleton, and M. Canals (2000), Evidence for enhanced Mediterranean thermohaline circulation during rapid climatic coolings, *Earth Planet. Sci. Lett.*, *183*, 417–429, doi:10.1016/S0012-821X(00)00296-X.

Cacho, I., J. O. Grimalt, M. Canals, L. Sbaffi, N. J. Shackleton, J. Schönfeld, and R. Zahn (2001), Variability of the western Mediterranean Sea surface temperature during the last 25,000 years and its connection with the Northern Hemisphere climatic changes, *Paleoceanography*, *16*, 40–52, doi:10.1029/2000PA000502.

Cacho, I., J. O. Grimalt, and M. Canals (2002), Response of the western Mediterranean Sea to rapid climatic variability during the last 50,000 years: A molecular biomarker approach, *J. Mar. Syst.*, *33–34*, 253–272, doi:10.1016/S0924-7963(02)00061-1.

Clark, P. U., S. J. Marshall, G. K. C. Clarke, S. W. Hostetler, J. M. Licciardi, and J. T. Teller (2001), Freshwater forcing of abrupt climate change during the last glaciation, *Science*, *293*, 283–287, doi:10.1126/science.1062517.

Clark, P. U., N. G. Pisias, T. F. Stocker, and A. J. Weaver (2002), The role of the thermohaline circulation in abrupt climate change, *Nature*, *415*, 863–869, doi:10.1038/415863a.

Clarke, G. K. C., D. W. Leverington, J. Teller, and A. S. Dyke (2004), Paleohydraulics of the last outburst flood glacial Lake Agassiz and the 8200 BP cold event, *Quat. Sci. Rev.*, *23*, 389–407, doi:10.1016/j.quascirev.2003.06.004.

Cranwell, P. A. (1973), Chain-length distribution of n-alkanes from lake sediments in relation to post-glacial environmental change, *Freshwater Biol.*, *3*, 259–265, doi:10.1111/j.1365-2427.1973.tb00921.x.

Cronin, T. M., G. S. Dwyer, T. Kamiya, S. Schwede, and D. A. Willard (2003), Medieval Warm Period, Little Ice Age and 20th century temperature variability from Chesapeake Bay, *Global Planet. Change*, *36*, 17–29, doi:10.1016/S0921-8181(02)00161-3.

Dahl-Jensen, D., K. Mosegaard, N. Gundestrup, G. D. Clow, S. J. Johnsen, A. W. Hansen, and N. Balling (1998), Past temperatures directly from the Greenland Ice Sheet, *Science*, *282*, 268–271, doi:10.1126/science.282.5387.268.

deMenocal, P., J. Ortiz, T. Guiderson, J. Adkins, M. Sarnthein, L. Baker, and M. Yarusinsky (2000a), Abrupt onset and termination of the African Humid Period: Rapid climate responses to gradual insolation forcing, *Quat. Sci. Rev.*, *19*, 347–361, doi:10.1016/S0277-3791(99)00081-5.

deMenocal, P., J. Ortiz, T. Guiderson, and M. Sarnthein (2000b), Coherent high- and low-latitude climate variability during the Holocene warm period, *Science*, *288*, 2198–2202, doi:10.1126/science.288.5474.2198.

Dias, J. M. A., T. Boski, A. Rodrigues, and F. Magalhães (2000), Coast line evolution in Portugal since the Last Glacial Maximum until present—A synthesis, *Mar. Geol.*, *170*, 177–186, doi:10.1016/S0025-3227(00)00073-6.

Diz, P., G. Francés, C. Pelejero, J. O. Grimalt, and F. Vilas (2002), The last 3000 years in the Ría the Vigo (NW Iberian Margin): Climatic and hydrographic signals, *Holocene*, *12*, 459–468, doi:10.1191/0959683602hl550rp.

Dokken, T. M., and E. Jansen (1999), Rapid changes in the mechanism of ocean convection during the last glacial period, *Nature*, *401*, 458–461, doi:10.1038/46753.

Eglinton, G., and R. J. Hamilton (1967), Leaf epicuticular waxes, *Science*, *156*, 1322–1335, doi:10.1126/science.156.3780.1322.

Ellison, C. R. W., M. R. Chapman, and I. R. Hall (2006), Surface and deep ocean interaction during the cold climate event 8200 years ago, *Science*, *312*, 1929–1932, doi:10.1126/science.1127213.

Fiúza, A. F. G. (1983), Upwelling patterns off Portugal, in *Coastal Upwelling: Its Sediment Records (Part A)*, edited by A. E. Suess and J. Thiede, pp. 85–98, Plenum, New York.

Flores, J. A., and F. J. Sierro (1997), Revised technique for calculation of calcareous nanofossil accumulation rates, *Micropaleontology*, *43*, 321–324, doi:10.2307/1485832.

Frigola, J., A. Moreno, I. Cacho, M. Canals, F. J. Sierro, J. A. Flores, J. O. Grimalt, D. A. Hodell, and J. H. Curtis (2007), Holocene climate variability in the western Mediterranean region from a deepwater record, *Paleoceanography*, *22*, PA2209, doi:10.1029/2006PA001307.

Gaspar, L. C., and J. H. Monteiro (1977), Matéria orgânica nos sedimentos da plataforma continental portuguesa entre os cabos Espichel e Raso, *Comun. Serv. Geol. Portugal*, *62*, 69–83, Lisbon.

Giraudeau, J., C. Michel, S. Manthé, L. Labeyrie, and G. Bond (2000), Coccolith evidence for instabilities in surface circulation south of Iceland during Holocene times, *Earth Planet. Sci. Lett.*, *179*, 257–268, doi:10.1016/S0012-821X(00)00113-8.

Grimalt, J. O., P. Fernández, J. Bayona, and J. Albaigés (1990), Assessment of fecal sterols and ketones as indicators of urban sewage input to coastal waters, *Environ. Sci. Technol.*, *24*, 357–363, doi:10.1021/es00073a011.

Grimalt, J. O., E. Calvo, and C. Pelejero (2001), Sea surface paleotemperature errors in $U_{37}^{K'}$ estimation due to alkenone measurements near the limit of detection, *Paleoceanography*, *16*, 226–232, doi:10.1029/1999PA000440.

Gupta, A. K., D. M. Anderson, and J. T. Overpeck (2003), Abrupt changes in the Asian southwest monsoon during the Holocene and their links to the North Atlantic Ocean, *Nature*, *421*, 354–357, doi:10.1038/nature01340.

Houghton, J. T., , Y. Dring, D. J. Griggs, M. Noguer, P. J. Van der Linden, and D. M. Xiaosu (Eds.) (2001), *Climate*

Change 2001: The Scientific Basis, p. 944, Cambridge Univ. Press, Cambridge, U. K.

Hughen, K. A., et al. (2004), Marine 04 marine radiocarbon age calibration, 26 - 0 ka BP, *Radiocarbon*, *46*, 1059–1086.

Hughes, M. K., and H. F. Diaz (1994), Was there a "Medieval Warm Period" and if so, where and when?, *Clim. Change*, *26*, 109–142, doi:10.1007/BF01092410.

Jackson, M. G., N. Oskarson, R. G. Trønnes, J. F. McManus, D. Oppo, K. Gröveld, S. R. Hart, and J. P. Sachs (2005), Holocene loess deposition in Iceland: Evidence for millennial scale atmosphere-ocean coupling in the North-Atlantic, *Geology*, *33*, 509–512, doi:10.1130/G21489.1.

Jansen, J. H. F., S. J. Van der Gaast, B. Koster, and A. J. Vaars (1998), Cortex, a shipboard XRF-scanner for element analyses in split sediment cores, *Mar. Geol.*, *151*, 143–153, doi:10.1016/S0025-3227(98)00074-7.

Johnsen, S. J., D. Dahl-Jensen, N. S. Gundestrup, J. P. Steffensen, H. B. Clausen, H. Miller, V. Masson-Delmotte, A. E. Sveinbjornsdottir, and J. W. C. White (2001), Oxygen isotope and palaeotemperature records from six Greenland ice-core stations: Camp Century, Dye-3, GRIP, GISP 2, Renland and NorthGRIP, *J. Quat. Sci.*, *16*, 299–307, doi:10.1002/jqs.622.

Jones, P. D., and M. E. Mann (2004), Climate over past millennia, *Rev. Geophys.*, *42*, RG2002, doi:10.1029/2003RG000143.

Jones, P. D., T. J. Osborn, and K. R. Briffa (2001), The evolution of climate over the last millennium, *Science*, *292*, 662–667, doi:10.1126/science.1059126.

Keigwin, L. (1996), The Little Ice Age and Medieval Warm Period in the Sargasso Sea, *Science*, *274*, 1503–1508, doi:10.1126/science.274.5292.1503.

Keigwin, L. D., J. P. Sachs, Y. Rosenthal, and E. A. Boyle (2005), The 8200 year B.P. event in the slope water system, western subpolar North Atlantic, *Paleoceanography*, *20*, PA2003, doi:10.1029/2004PA001074.

Kim, J.-H., N. Rimbu, S. J. Lorenz, G. Lohmann, S.-I. Nam, S. Schouten, C. Rühlemann, and R. R. Schneider (2004), North Pacific and North Atlantic sea-surface temperature variability during the Holocene, *Quat. Sci. Rev.*, *23*, 2141–2154, doi:10.1016/j.quascirev.2004.08.010.

Kleiven, H. K. F., C. Kissel, C. Laj, U. S. Ninnemann, T. O. Richter, and E. Cortijo (2008), Reduced North Atlantic deep water coeval with the glacial lake Agassiz freshwater outburst, *Science*, *319*, 60–64, doi:10.1126/science.1148924.

Knudsen, K. L., H. Jiang, E. Jansen, J. Eiriksson, J. Heinemeier, and M. S. Seidenkrantz (2004), Environmental changes off north Iceland during the deglaciation and the Holocene: Foraminifera, diatoms and stable isotopes, *Mar. Micropaleontol.*, *50*, 273–305, doi:10.1016/S0377-8398(03)00075-6.

Lamb, H. H. (1985), *Climate History and the Future*, 835 pp., Princeton Univ. Press, Princeton, N. J.

Lambeck, K., and J. Chappell (2001), Sea level change through the last glacial cycle, *Science*, *292*, 679–686, doi:10.1126/science.1059549.

Lebreiro, S. M., et al. (2006), Climate change and coastal hydrographic response along the Atlantic Iberian margin (Tagus Prodelta and Muros Ría) during the last two millennia, *Holocene*, *16*, 1003–1015, doi:10.1177/0959683606hl990rp.

Leduc, G., L. Vidal, K. Tachikawa, F. Rostek, C. Sonzogni, L. Beaufort, and E. Bard (2007), Moisture transport across Central America as a positive feedback on abrupt climatic changes, *Nature*, *445*, 908–911, doi:10.1038/nature05578.

Liu, J. P., J. D. Milliman, S. Gao, and P. Cheng (2004), Holocene development of the Yellow River's subaqueous delta North Yellow Sea, *Mar. Geol.*, *209*, 45–67, doi:10.1016/j.margeo.2004.06.009.

Lorenz, S. J., J.-H. Kim, N. Rimbu, and R. R. Schneider (2006), Orbitally driven insolation forcing on Holocene climate trends: Evidence from alkenone data and climate modeling, *Paleoceanography*, *21*, PA1002, doi:10.1029/2005PA001152.

Marchal, O., I. Cacho, T. F. Stocker, J. O. Grimalt, E. Calvo, and B. Martrat (2002), Apparent long-term cooling of the sea surface in the northeast Atlantic and Mediterranean during the Holocene, *Quat. Sci. Rev.*, *21*, 455–483, doi:10.1016/S0277-3791(01)00105-6.

Maslin, M., and S. J. Burns (2000), Reconstruction of the Amazon Basin effective moisture availability over the past 14,000 years, *Science*, *290*, 2285–2287, doi:10.1126/science.290.5500.2285.

Mateus, J. E. R. R. (1992), *Holocene and Present-Day Ecosystems of the Carvalhal Region, Southwest Portugal*, 184 pp., Rijks Univ., Utrecht, Netherlands.

Mayewski, P. A., et al. (2004), Holocene climate variability, *Quat. Res.*, *62*, 243–255, doi:10.1016/j.yqres.2004.07.001.

McManus, J. F., D. W. Oppo, and J. L. Cullen (1999), A 0.5-million-year record of millennial-scale climate variability in the North Atlantic, *Science*, *283*, 971–975, doi:10.1126/science.283.5404.971.

Moita, M. T. (2001), *Estrutura Variabilidade e Dinâmica do Fitoplânton na Costa de Portugal Continental*, 272 pp., Fac. de Ciênc. de Lisboa, Lisbon.

Monteiro, J. H., A. Voelker, A. Ferreira, M. Mil-Homens, S. Nave, V. Magalhães, E. Salgueiro, S. Vaqueiro, S. Muiños, and P. Freitas (2002), Report of the cruise PALEO I (PO287) on FS Poseidon (April 22–May 3, 2002), technical report, 78 pp., Inst. Geol. e Mineiro, Alfragide, Portugal.

Müller, C., and R. Stein (2000), Variability of fluvial sediment supply to the Laptev Sea continental margin during Late Weichselian to Holocene times: Implications from clay-mineral records, *Int. J. Earth Sci.*, *89*, 592–604, doi:10.1007/s005310000112.

Müller, P., G. Kirst, G. Ruhland, I. v. Storch, and A. Rosell-Melé (1998), Calibration of the alkenone index Uk′37 based on core-tops from the eastern South Atlantic and global ocean (60°N–60°S), *Geochim. Cosmochim. Acta*, *62*, 1757–1772, doi:10.1016/S0016-7037(98)00097-0.

Naughton, F., J.-F. Bourillet, M. F. Sánchez-Goñi, J.-L. Turon, and J.-M. Jouanneau (2007a), Long-term and millennial-scale climate variability in northwestern France during the last 8850 years, *Holocene*, *17*, 939–953, doi:10.1177/0959683607082410.

Naughton, F., M. F. Sánchez-Goñi, S. Desprat, J.-L. Turon, J. Duprat, B. Malaizé, C. Joly, E. Cortijo, T. Drago, and M. C. Freitas (2007b), Present-day and past (last 25000 years) marine pollen signal off western Iberia, *Mar. Micropaleontol.*, *62*, 91–114.

North Greenland Ice Core Project Members (2004), High resolution record of Northern Hemisphere climate extending into the last interglacial period, *Nature*, *431*, 147–151, doi:10.1038/nature02805.

O'Brien, S. R., P. A. Mayewski, L. D. Meeker, D. A. Meese, M. S. Twickler, and S. I. Whitlow (1995), Complexity of Holocene climate as reconstructed from a Greenland ice core, *Science*, *270*, 1962–1964, doi:10.1126/science.270.5244.1962.

Poynter, J., and G. Eglinton (1990), Molecular composition of three sediments from Hole 717C: The Bengal Fan, *Proc. Ocean Drill. Program Sci. Results*, *116*, 155–161.

Queiroz, P. F. (1999), *Ecologia Histórica Da Paisagem do Nordeste Alentejano*, 300 pp., Univ. de Lisboa, Lisbon.

Rasmussen, S. O., et al. (2006), A new Greenland ice core chronology for the last glacial termination, *J. Geophys. Res.*, *111*, D06102, doi:10.1029/2005JD006079.

Rivera, J., E. B. Karabanov, D. F. Williams, V. Buchinskyi, and M. Kuzmin (2006), Lena River discharge events in sediments of Laptev Sea, Russian Arctic, *Estuarine Coastal Shelf Sci.*, *66*, 185–196, doi:10.1016/j.ecss.2005.08.009.

Rohling, E., and H. Pälike (2005), Centennial-scale climate cooling with a sudden cold event around 8,200 years ago, *Nature*, *434*, 975–979, doi:10.1038/nature03421.

Roucoux, K. H., P. C. Tzedakis, L. Abreu, and N. Shacketon (2006), Climate and vegetation changes 180000 to 345000 years ago recorded in a deep-sea core off Portugal, *Earth Planet. Sci. Lett.*, *249*, 307–325, doi:10.1016/j.epsl.2006.07.005.

Ruddiman, W. F., and A. McIntyre (1981), The mode and mechanism of the last deglaciation: Oceanic evidence, *Quat. Res.*, *16*, 125–134, doi:10.1016/0033-5894(81)90040-5.

Sánchez-Goñi, M. F., I. Cacho, J. L. Turon, J. Guiot, F. J. Sierro, J.-P. Peypouquet, J. O. Grimalt, and N. J. Shackleton (2002), Synchroneity between marine and terrestrial responses to millennial scale climatic variability during the last glacial period in the Mediterranean region, *Clim. Dyn.*, *19*, 95–105, doi:10.1007/s00382-001-0212-x.

Sarnthein, M., S. Van Kreveld, H. Erlenkeuser, P. M. Grootes, M. Kucera, U. Pflaumann, and M. Schulz (2003), Centennial-to-millennial-scale periodicities of Holocene climate and sediment injections off the western Barents shelf, 75°N, *Boreas*, *32*(3), 447–461, doi:10.1080/03009480310003351.

Schefuß, E., S. Schouten, and R. Schneider (2005), Climatic controls on central African hydrology during the past 20,000 years, *Nature*, *437*, 1003–1006, doi:10.1038/nature03945.

Schubert, S. J., J. Villanueva, S. E. Calvert, G. L. Cowie, U. VonRad, H. Schulz, and U. Berber (1998), Stable phytoplankton community in the Arabian Sea over the last 200,000 years, *Nature*, *394*, 563–566, doi:10.1038/29047.

Schulte, S., F. Rostek, E. Bard, J. Rullkoetter, and O. Marchal (1999), Variations of oxygen-minimum and primary productivity record in sediments of the Arabian Sea, *Earth Planet. Sci. Lett.*, *173*, 205–221, doi:10.1016/S0012-821X(99)00232-0.

Siddall, M., E. J. Rohling, A. Almogi-Labin, C. Hemleben, D. Meischner, I. Schmeizer, and D. A. Smeed (2003), Sea-level fluctuations during the last glacial cycle, *Nature*, *423*, 853–858, doi:10.1038/nature01690.

Siddall, M., D. A. Smeed, C. Hemleben, E. J. Rohling, I. Schmelzer, and W. R. Peltier (2004), Understanding the Red Sea response to sea level, *Earth Planet. Sci. Lett.*, *225*, 421–434, doi:10.1016/j.epsl.2004.06.008.

Siddall, M., E. Bard, E. J. Rohling, and C. Hemleben (2006), Sea-level reversal during Termination II, *Geology*, *34*, 817–820, doi:10.1130/G22705.1.

Stein, R., et al. (2004), Arctic (palaeo) river discharge and environmental change: Evidence from Holocene Kara Sea sedimentary records, *Quat. Sci. Rev.*, *23*, 1485–1511, doi:10.1016/j.quascirev.2003.12.004.

Storms, J. E. A., R. M. Hoogendoorn, R. A. C. Dam, A. J. F. Hoitink, and S. B. Kroonenberg (2005), Late-Holocene evolution of the Mahakam delta, East Kalimantan, Indonesia, *Sediment. Geol.*, *180*, 149–166, doi:10.1016/j.sedgeo.2005.08.003.

Stuiver, M., and P. J. Reimer (1993), Extended 14C data base and revised CALIB radiocarbon calibration program, *Radiocarbon*, *35*, 215–230.

Stuiver, M., P. J. Reimer, E. Bard, W. J. Beck, G. S. Burr, A. Hughen, B. Kromer, F. G. M. Cormac, J. Van der Plicht, and M. Spurk (1998), INTCAL98 radiocarbon age calibration, 24000 cal BP, *Radiocarbon*, *40*, 1041–1083.

Tanabe, S., Y. Saito, Q. Lan Vu, T. J. J. Hanebuth, Q. Lan Ngo, and A. Kitamura (2006), Holocene evolution of the Song Hong (Red River) delta system, northern Vietnam, *Sediment. Geol.*, *187*, 29–61, doi:10.1016/j.sedgeo.2005.12.004.

Tareq, S. M., E. Tanoue, H. Tsuji, N. Tanaka, and K. Ohta (2005), Hydrocarbon and elemental carbon signatures in a tropical wetland: Biogeochemical evidence of forest fire vegetation changes, *Chemosphere*, *59*, 1655–1665, doi:10.1016/j.chemosphere.2005.02.019.

Teller, J. T., D. W. Leverington, and J. D. Mann (2002), Freshwater outbursts to the ocean from glacial Lake Agassiz and their role in climate change during the last deglaciation, *Quat. Sci. Rev.*, *21*, 879–887, doi:10.1016/S0277-3791(01)00145-7.

Trigo, R., and C. C. DaCamara (2000), Circulation weather types and influence on the precipitation regime in Portugal, *Int. J. Climatol.*, *20*, 1559–1581, doi:10.1002/1097-0088(20001115)20:13<1559::AID-JOC555>3.0.CO;2-5.

Trigo, R. M., T. J. Osborn, and J. Corte-Real (2002), The North Atlantic Oscillation influence on Europe: Climate impacts and associated physical mechanisms, *Clim. Res.*, *20*, 9–17, doi:10.3354/cr020009.

Turon, J. L., A.-M. Lézine, and M. Denèfle (2003), Land-sea correlations for the last glaciation inferred from a pollen and dinocyst record from the Portuguese Margin, *Quat. Res.*, *59*, 88–96, doi:10.1016/S0033-5894(02)00018-2.

Vale, C. (1981), Entrada de matéria em suspensão no estuário do Tejo durante as chuvas de Fevereiro de 1979, *Recur. Hídricos*, *2*, 37–45.

Van der Knaap, W. O., and J. F. N. Van Leeuwen (1985), Holocene vegetation succession and degradation as response to climatic change and human activity in the Serra da Estrela, Portugal, *Rev. Palaeobot. Palynol.*, *89*, 153–211.

Villanueva, J., C. Pelejero, and J. O. Grimalt (1997), Clean-up procedures for the unbiased estimation of C_{37} alkenone sea surface temperatures and terrigenous *n*-alkane in paleoceanography, *J. Chromatogr. A*, *757*, 145–151, doi:10.1016/S0021-9673(96)00669-3.

Villanueva, J., J. O. Grimalt, L. D. Labeyrie, E. Cortijo, L. Vidal, and J. Louis-Turon (1998), Precessional forcing of productivity in the North Atlantic Ocean, *Paleoceanography*, *13*, 561–571, doi:10.1029/98PA02318.

Villanueva, J., E. Calvo, C. Pelejero, J. O. Grimalt, A. Boelaert, and L. Labeyrie (2001), A latitudinal productivity band in the central North Atlantic over the last 270 kyr: An alkenone perspective, *Paleoceanography*, *16*, 617–626, doi:10.1029/2000PA000543.

Vis, G.-J., C. Kasse, and J. Van Denberghe (2008), Late Pleistocene and Holocene palaeogeography of the Lower Tagus Valley (Portugal): Effects of relative sea level, valley morphology and sediment supply, *Quat. Sci. Rev.*, *27*, 1682–1709, doi:10.1016/j.quascirev.2008.07.003.

Weijers, J. W. H., E. Schefuß, S. Schouten, and J. S. S. Damsté (2007), Coupled thermal and hydrological evolution of tropical Africa over the last deglaciation, *Science*, *315*, 1701–1704, doi:10.1126/science.1138131.

Weldeab, S., R. R. Schneider, and M. Kölling (2006), Deglacial sea surface temperature and salinity increase in the western tropical Atlantic in synchrony with high latitude climate instabilities, *Earth Planet. Sci. Lett.*, *241*, 699–706, doi:10.1016/j.epsl.2005.11.012.

Weldeab, S., D. W. Lea, R. R. Schneider, and N. Andersen (2007), 155,000 years of West African monsoon and ocean thermal evolution, *Science*, *316*, 1303–1307, doi:10.1126/science.1140461.

Wells, P., and H. Okada (1997), Response of nannoplankton to major changes in sea-surface temperature and movements of hydrological fronts over Site DSDP 594 (south Chatham Rise, southeast New Zealand) during the last 130ky, *Mar. Micropaleontol.*, *32*, 341–363, doi:10.1016/S0377-8398(97)00025-X.

Winter, A., R. W. Jordan, and P. H. Roth (1994), Biogeography of living coccolithophores in ocean waters, in *Coccolithophores*, edited by A. Winter and W. G. Siesser, pp. 161–177, Cambridge Univ. Press, Cambridge, U. K.

Xiao, S., A. Li, J. P. Liu, M. Chen, Q. Xie, F. Jiang, T. Li, R. Xiang, and Z. Chen (2006), Coherence between solar activity and the East Asian winter monsoon variability in the past 8000 years from Yangtze River-derived mud in the East China Sea, *Palaeogeogr. Palaeoclimatol. Palaeoecol.*, *237*, 293–304, doi:10.1016/j.palaeo.2005.12.003.

Xu, J., W. Kuhnt, A. Holbourn, N. Andersen, and G. Bartoli (2006), Changes in the vertical profile of the Indonesian Throughflow during Termination II: Evidence from the Timor Sea, *Paleoceanography*, *21*, PA4202, doi:10.1029/2006PA001278.

Yokoyama, Y., P. De Deckker, K. Lambeck, P. Johnston, and L. K. Fifield (2000), Timing of the Last Glacial Maximum from observed sea-level minima, *Nature*, *406*, 713–716, doi:10.1038/35021035.